

pinning (which are not understood at present).

When the external magnetic field is swept at a constant rate  $dH_0/dt$  and no ac magnetic field is superimposed on the swept field, one measures a voltage which is proportional to  $dM/dH_0$ . In other words, one measures the slope of the static magnetization curve directly.<sup>3</sup> When a time-varying field  $h_0 \sin \omega t$  is superimposed on the swept field<sup>9</sup> the interpretation of the experimental results is more complex, though the physics of the superconducting surface sheath is the same as has been discussed above.

I would like to thank L. J. Barnes for interesting discussions.

Note added in proof.—Recent experiments by P. O. J. Van Engelen, G. J. C. Bots, and B. S. Blaisse [Phys. Letters 19, 465 (1965)] and also by E. Maxwell and W. P. Robbins (to be published) came to the author's attention. These experiments can be readily interpreted with the above theory.

\*Based on work sponsored by the Research for Metallurgy and Materials Progress, Division of Research,

U. S. Atomic Energy Commission, under Contact No. AT-(11-1)-GEN-8.

<sup>1</sup>M. Strongin, A. Paskin, D. G. Schweitzer, O. F. Kammerer, and P. P. Craig, Phys. Rev. Letters **12**, 442 (1964).

<sup>2</sup>D. J. Sandiford and D. G. Schweitzer, Phys. Letters **13**, 98 (1964).

<sup>3</sup>L. J. Barnes and H. J. Fink, to be published.

<sup>4</sup>H. J. Fink and L. J. Barnes, Phys. Rev. Letters **15**, 792 (1965).

<sup>5</sup>When  $H_0$  is kept constant and  $h_0$  is slowly reduced from  $h_c$  to zero, the  $4\pi M$  value of the sample will approximately vanish. The total current in the sheath is then zero and the sample is "demagnetized."

<sup>6</sup>For simplicity we have linearized the  $\pm 4\pi M$  curves and the  $h_i(t)$  curve. This is a good approximation for samples of the size used in Ref. 1.

<sup>7</sup>L. D. Landau and E. M. Lifshitz, Electrodynamics of Continuous Media, (Addison-Wesley Publishing Company, Inc., Reading, Massachusetts, 1960), p. 194; N. W. MacLachlin, Bessel Functions for Engineers (Clarendon Press, Oxford, England, 1955), 2nd ed., p. 165; E. Maxwell and M. Strongin, Phys. Rev. Letters **10**, 212 (1963).

<sup>8</sup>H. J. Fink, Phys. Rev. Letters **14**, 309 (1965); H. J. Fink and R. D. Kessinger, Phys. Rev. **140**, A1937 (1965).

<sup>9</sup>M. Strongin, D. G. Schweitzer, A. Paskin, and P. P. Craig, Phys. Rev. **136**, A926 (1964).

## NEAR-FORWARD RAMAN SCATTERING IN ZINC OXIDE

S. P. S. Porto, B. Tell, and T. C. Damen

Bell Telephone Laboratories, Murray Hill, New Jersey

(Received 2 February 1966)

In polar crystals, electromagnetic waves and optical phonons interact strongly when their energies and wave vectors are nearly equal. This interaction removes the intersection of the uncoupled dispersion curves,<sup>1</sup> and results in an upper and lower branch which have mixed electromagnetic and mechanical nature. The crystal excitations in this mixed region have been called polaritons by Henry and Hopfield<sup>2</sup> who were the first to observe Raman scattering from them. Henry and Hopfield observed a 20% shift in the polariton frequency in GaP as the scattering angle was varied from the forward to near-forward direction.

Because ZnO is a uniaxial crystal, we have been able to obtain nearly a three-fold shift in the polariton frequency as a function of angle in the near-forward direction. The advantage of a uniaxial crystal<sup>3</sup> is that in a positive crystal such as ZnO the frequency of the polar-

iton that conserves energy and wave vector can be made small if one makes the incident light an ordinary ray and the Stokes Raman light an extraordinary ray with the maximum index. The frequency of the allowed polariton is increased as the angle from the forward direction is increased, so that a frequency shift from 160 to 407  $\text{cm}^{-1}$  has been obtained.

For comparison, the case in which the input is an extraordinary ray with the maximum index and the Raman light is an ordinary ray has also been studied. Here, the wave vector and therefore the frequency of allowed polariton is large in the forward direction, so that a shift of only around 20% in the polariton frequency was obtained.

Our experimental setup consists of the ordinary (extraordinary) incident light (4880 Å from the ionized argon laser) propagating along the  $x$  axis while the extraordinary (ordinary)

Stokes light is detected in the  $xz$  plane at an angle  $\theta$  from the incident light. The case in which the input is ordinary is termed  $(yz)$ , and in which the input is extraordinary is  $(zy)$ . In both cases, the polariton is transverse ordinary and polarized along the  $y$  axis.<sup>4</sup> The scattered light is accepted with approximately a  $0.5^\circ$  (in the crystal) acceptance angle, passes through a double-grating spectrometer, and is photoelectrically detected. The finite acceptance angle was necessitated by intensity considerations.

The dispersion curves for the transverse ordinary excitations are calculated using the standard formula from Born and Huang:

$$\frac{k^2}{\omega^2/c^2} = \frac{\nu_0^2 \epsilon_{\perp}^0 - \nu_{\perp}^2 \epsilon_{\perp}^{\infty}}{\nu_0^2 - \nu^2}, \quad (1)$$

where the two solutions for a given wave vector  $k$  yield the two branches of the dispersion curve, i.e., the two values of  $\omega = 2\pi\nu$ . Here,  $\nu_0$  is the lattice dispersion frequency at  $407 \text{ cm}^{-1}$ ,<sup>5</sup>  $\epsilon_{\perp}^0$  and  $\epsilon_{\perp}^{\infty}$  are the static and high-frequency dielectric constants and are taken as 8.15 and 4.0, respectively.<sup>6</sup> The calculated lower dispersion curve, obtained from Eq. (1), is shown as the solid lines in Fig. 1.

Energy and wave-vector conservation for small  $\theta$  give

$$k = \{[\nu_l(n_e - n_o) + \nu n_o]^2 + \nu_l(\nu_l - \nu)n_e n_o \theta^2\}^{1/2} \quad (2a)$$

for the input extraordinary and the output ordinary  $(yz)$ , and

$$k = -\{[\nu n_e - \nu_l(n_e - n_o)]^2 + \nu_l(\nu_l - \nu)n_e n_o \theta^2\}^{1/2} \quad (2b)$$

for the input ordinary and the output extraordinary  $(zy)$ . Here  $\nu_l$  is the laser frequency, and  $n_o$  and  $n_e$  are the ordinary and extraordinary refractive indices obtained by interpolation of values from Bond.<sup>7</sup>  $k$  is plotted in units of  $2\pi\nu_0/c$  and its sign is determined from physical considerations at  $\theta = 0$ . It is convenient to plot the  $(yz)$  case separate from the  $(zy)$ , so the sign is maintained even for  $\theta \neq 0$ .

The energy-wave-vector conservation curves for various angles are shown as dashed lines in Fig. 1, with the experimental points. The bars indicate the width at half-maximum of the Raman lines due to the finite solid angle. The smaller angle Raman lines are broader since the frequency changes faster as a function of angle. In Fig. 2 are shown the recorder traces for the Raman scattered light for the  $(yz)$  case,

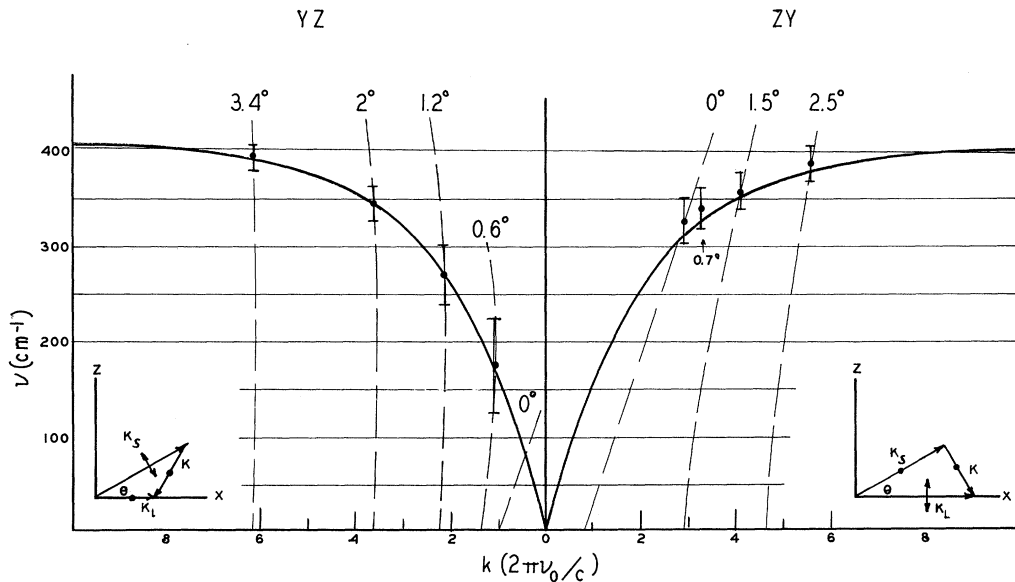


FIG. 1. The theoretical dispersion curves for ZnO are the solid lines, while the dashed lines are the polariton energy and wave-vector conservation conditions for a given angle. The intersections yield the allowed polaritons. The experimental points are the circles, and the bars indicate the linewidth at half-maximum. The inserts give the kinematics for the two cases. The single arrows are the propagation directions, while the double arrows and dots indicate polarizations in and normal, respectively, to the plane of propagation. Here,  $k_l, k_s$ , and  $k$  are the wave vectors of the laser light, Stokes light, and polariton, respectively.

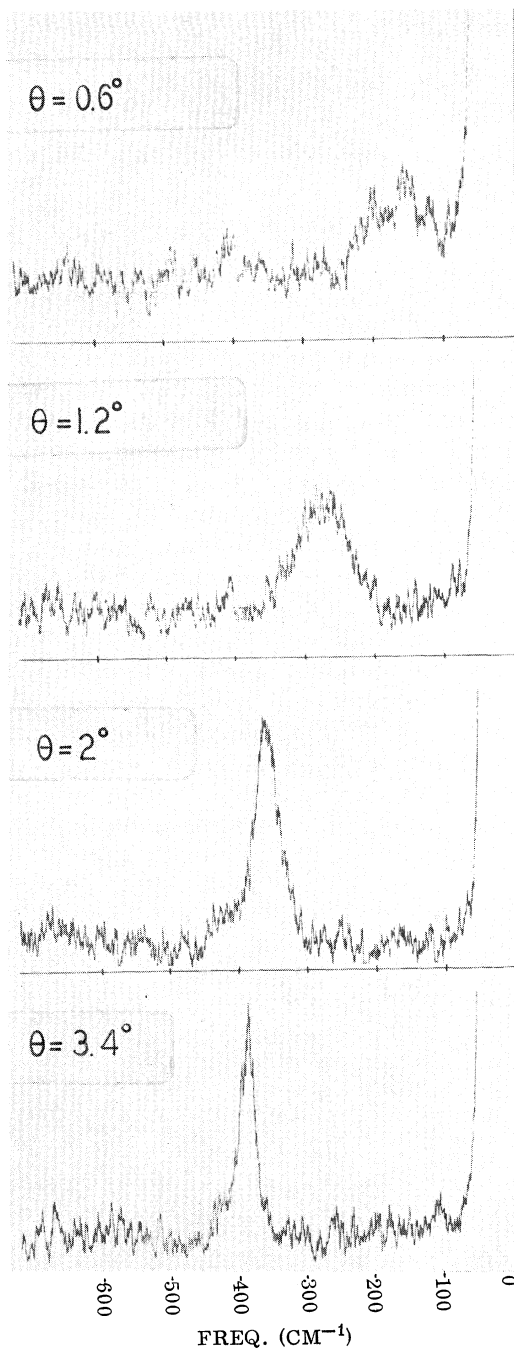


FIG. 2. Recorder traces of the Raman effect for the (yz) case for various angles.

where the sharpening of the lines and the frequency shift as  $\theta$  increases are pronounced. The presence and increasing intensity of argon-emission lines and of the exciting line prevented a determination of the polariton frequency closer to the exact forward direction.

A Raman shift due to polaritons on the upper branch was expected to occur in the forward direction for the (yz) case starting near  $850 \text{ cm}^{-1}$ . This line was expected to be broad since in the region where this branch satisfies the conservation conditions, its frequency changes rapidly as a function of angle. Unfortunately, we have not been able to detect any scattering from this branch.

In conclusion, we have been able to plot a sizable portion of the lower dispersion curve in ZnO in good agreement with theory. Furthermore, we have found that the strength of the Raman scattering does not change appreciably as the polariton character changes from mostly electromagnetic to mechanical, although the electron-polariton coupling changes from an electromagnetic to a deformation potential.

We wish to thank E. Kolb for supplying some of the crystals used in this work, and R. J. Martin for sample preparation. We also wish to thank S. J. Buchsbaum, J. P. Gordon, and C. H. Henry for comments on the manuscript.

<sup>1</sup>K. Huang, Proc. Roy. Soc. (London) **A208**, 352 (1951); M. Born and K. Huang, *Dynamical Theory of Crystal Lattices* (Oxford University Press, New York, 1956), pp. 89 ff.

<sup>2</sup>C. H. Henry and J. J. Hopfield, Phys. Rev. Letters **15**, 964 (1965).

<sup>3</sup>R. Loudon, Proc. Phys. Soc. (London) **82**, 393 (1963).

<sup>4</sup>The polariton polarization is determined from the polarizability tensors for a  $C_{6V}$  crystal as given by R. Loudon, Advan. Phys. **13**, 423 (1964). Furthermore, the extraordinary polariton in the forward direction can only be observed for the incident and Stokes light both ordinary or both extraordinary.

<sup>5</sup>T. C. Damen, S. P. S. Porto, and B. Tell, Phys. Rev. **142**, 570 (1966).

<sup>6</sup>R. J. Collins and D. A. Kleinman, Phys. Chem. Solids **11**, 190 (1959).

<sup>7</sup>W. L. Bond, J. Appl. Phys. **36**, 1674 (1965).

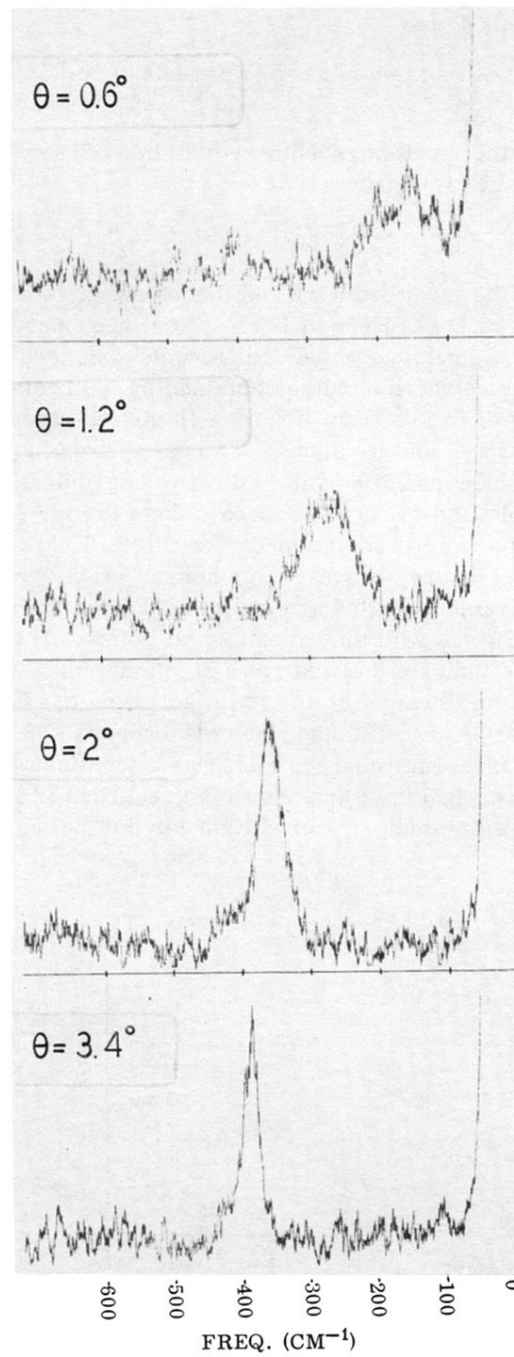


FIG. 2. Recorder traces of the Raman effect for the (yz) case for various angles.